VIROLOGY

Single-dose VSV-based vaccine protects against Kyasanur Forest disease in nonhuman primates

Bharti Bhatia[1]†, Tsing-Lee Tang-Huau[1]‡, Friederike Feldmann[2], Patrick W. Hanley[2], Rebecca Rosenke[2], Carl Shaia[2], Andrea Marzi[1], Heinz Feldmann[1]*

Kyasanur Forest disease virus (KFDV) is an endemic arbovirus in western India mainly transmitted by hard ticks of the genus *Haemaphysalis*. KFDV causes Kyasanur Forest disease (KFD), a syndrome including fever, gastrointestinal symptoms, and hemorrhages. There are no approved treatments, and the efficacy of the only vaccine licensed in India has recently been questioned. Here, we studied the protective efficacy of a vesicular stomatitis virus (VSV)–based vaccine expressing the KFDV precursor membrane and envelope proteins (VSV-KFDV) in pigtailed macaques. VSV-KFDV vaccination was found to be safe and elicited strong humoral and cellular immune responses. A single-dose vaccination reduced KFDV loads and pathology and protected macaques from KFD-like disease. Furthermore, VSV-KFDV elicited cross-reactive neutralizing immune responses to Alkhurma hemorrhagic fever virus, a KFDV variant found in Saudi Arabia.

INTRODUCTION

Kyasanur Forest disease virus (KFDV) is an emerging tick-borne flavivirus endemic in parts of western India. KFDV can cause a severe clinical syndrome with chills, fever, headache, myalgia, vomiting, gastrointestinal symptoms, and hemorrhages known as Kyasanur Forest disease (KFD). A subset of patients may develop a biphasic illness including recurring fever with or without neurological symptoms (*1*–*3*). It is estimated that up to 500 human KFDV infections occur annually with a case fatality rate of 3 to 5% (*1*–*4*). Because of its life-threatening pathogenicity and the absence of effective countermeasures, KFDV is classified as a Biosafety level 4 (BSL4) pathogen and, in the United States, as a select agent (*5*).

Hard ticks of the genus *Haemaphysalis* are vectors for KFDV with the main vector being *Haemaphysalis spinigera* (*2*). These ticks ingest vertebrate blood meals during different development stages, acquiring/transmitting KFDV to different avian and mammalian hosts as well as from tick-to-tick through co-feeding. Asymptomatic replication of KFDV has been reported from most avian and mammalian hosts including birds, cattle, and bats (*2*, *6*). Human KFDV infections occur mostly through tick bites during spring and summer seasons, which overlap with peak activity of adult *H. spinigera* (*7*).

Apart from humans, natural KFDV infections cause severe disease in some nonhuman primate species such as red-faced bonnet macaques (*Macaca radiata*) and black-faced langures (*Presbytis entellus*) (*2*, *4*). Symptomatic infection can be achieved experimentally in immunocompetent and immunodeficient mice, which serve as small-animal models for KFDV (*4*, *8*). Recently, a nonhuman primate model was established using pigtailed macaques (*Macaca nemestrina*) presenting with KFDV viremia and clinical disease recapitulating hallmark features of human KFD including flushed appearance, piloerection, dehydration, loss of appetite, weakness, and hemorrhagic signs (*9*). The pigtailed macaque represents an important animal disease model for countermeasure development against KFD.

The KFDV genome consists of a positive-sense, single-stranded RNA of 10,774 nucleotides (nt) that encodes a single polyprotein cleaved into three structural proteins [capsid, precursor membrane protein (prM), and envelope protein (E)] and seven non-structural proteins (*10*–*12*). Besides live-attenuated vaccines for yellow fever and Japanese encephalitis virus, vaccine development for flaviviruses such as Dengue and Zika virus is based on a variety of platforms mainly utilizing the structural proteins prM and E as immunogens (*13*–*20*).

In the past, India has used a formalin-inactivated whole virus vaccine to prevent KFDV infections (*21*). However, even with multiple booster immunizations, vaccinees still develop viremia and clinical illness following KFDV infection demonstrating limited vaccine efficacy (*21*). The future use of this vaccine has recently been questioned (*22*, *23*) leaving the public health response vulnerable to an emerging infectious disease. With increasing case numbers and the expansion of its endemicity, KFDV is considered an emerging regional public health concern on the Indian subcontinent. In addition, Alkhurma hemorrhagic fever virus (AHFV), a variant of KFDV, is of considerable emerging disease concern in Saudi Arabia and potentially other countries (*24*). Thus, the development of a cross-reactive and effective KFDV vaccine candidate is becoming of high importance for countries bordering the Arabian Sea (*6*).

Recently, we developed two versions of a KFDV vaccine candidate based on the vesicular stomatitis virus Ebola vaccine (VSV-EBOV) (*25*) additionally expressing the KFDV prM and E proteins (VSV-KFDV) (*26*). Both live-attenuated recombinant VSV vectors, which differ only in their EBOV glycoprotein (GP) gene (full-length versus truncated), provided strong protection against disease in BALB/c mice challenged with a lethal dose of KFDV. Protection

[1]Laboratory of Virology, Division of Intramural Research, National Institute of Allergy and Infectious Diseases, National Institutes of Health, Rocky Mountain Laboratories, Hamilton, MT, USA. [2]Rocky Mountain Veterinary Branch, Division of Intramural Research, National Institute of Allergy and Infectious Diseases, National Institutes of Health, Rocky Mountain Laboratories, Hamilton, MT, USA.
*Corresponding author. Email: feldmannh@niaid.nih.gov
†Present address: NextGen Invitro Diagnostics, RCB Campus Faridabad, Haryana 121003, India.
‡Present address: Sanofi Pasteur VaxDesign Corporation Research Services, 2501 Discovery Dr., Orlando, FL 32826, USA.

by these VSV-based vaccines was most likely mediated through antibodies as evidenced by passive transfer studies (*26*).

Here, we used the slightly more potent VSV vector expressing the full-length EBOV GP and the KFDV prM and E proteins, here designated VSV-KFDV, for evaluation of protection in the recently established pigtailed macaque model. We demonstrated that a single intramuscular vaccination with VSV-KFDV was safe and elicited specific and potent humoral and cellular immune responses. VSV-KFDV vaccination strongly reduced KFDV loads and uniformly protected macaques from disease following KFDV challenge. We also demonstrated that the humoral immune response elicited by VSV-KFDV potently neutralized AHFV infection in vitro. We conclude that VSV-KFDV is a promising second-generation KFDV vaccine candidate ready to enter clinical trials.

RESULTS

Study design

Ten female pigtailed macaques (*M. nemestrina*) were randomly assigned to either the control (tables S1 and S2, KFDV 1 to 4) or the study (tables S1 and S2, KFDV 5 to 10) group and vaccinated once intramuscularly with VSV-EBOV [1×10^7 plaque-forming units (PFU)] or VSV-KFDV (1×10^7 PFU), respectively (fig. S1). No adverse events were observed in the vaccinated animals except for one macaque (KFDV 5) that developed temporary muscle firmness at the vaccination site, a condition that resolved quickly without medical intervention. Later histopathological evaluation of the vaccination site of this animal showed no pathology. On D0 (28 days post-vaccination), macaques were challenged with KFDV [2×10^5 median tissue culture infectious dose ($TCID_{50}$)] via the combined subcutaneous and intravenous routes. Venous blood draws and physical examinations were performed on D0, D1, D3, D6, and D9 after KFDV challenge (fig. S1). Because this is not a lethal model with animals clearing virus and recovering from disease, we humanely euthanized all macaques on D9 to enable analysis of important disease parameters such as hematology, blood chemistry organ/blood loads, and histopathology to demonstrate vaccine efficacy.

VSV-KFDV vaccine induced antigen-specific humoral immune responses

Serum samples from vaccinated animals were analyzed for the presence of KFDV-specific immunoglobulin G (IgG) antibodies before (D−28, D−27, D−25, D−18, and D0) and after KFDV challenge (D1, D3, D6, and D9). All VSV-KFDV vaccinated animals seroconverted to KFDV-prM and -E antigens between D−18 and D0 with titers >1:100 at D0. Post-challenge titers increased to around 4 $\log_{10}$, indicating an anamnestic response to KFDV infection (Fig. 1A). Similarly, initial neutralizing antibody titers in VSV-KFDV vaccinated animals were detected at D0 ranging from 1:50 to 1:200 with titers increasing after challenge to >3 $\log_{10}$, again representing an anamnestic response to KFDV infection (Fig. 1B). Some VSV-EBOV vaccinated animals developed low-level IgG antibodies to KFDV-prM-E starting at D6 as a response to KFDV challenge but neutralizing antibodies to KFDV were not detected in these animals (Fig. 1, A and B). Humoral immune responses were also tested against AHFV, a KFDV variant. All VSV-KFDV vaccinated animals showed AHFV cross-reactive IgG antibodies starting at D0 with a titer around 1:100. The titers increased to up to 5 $\log_{10}$ following KFDV challenge (fig. S2A). Some VSV-EBOV vaccinated animals developed AHFV cross-reactive IgG antibodies by the time of euthanasia (fig. S2A). Similarly, neutralizing antibodies against AHFV were detected in all VSV-KFDV but not in VSV-EBOV vaccinated animals (fig. S2B). Overall, the kinetics and strength of the cross-reactive humoral immune response to AHFV were very similar to the humoral response to KFDV (Fig. 1, A and B). All study animals seroconverted to EBOV GP as expected (fig. S1C). Peak IgG responses were reached at D−18 with titers of ~3.5 to 4 $\log_{10}$, which did not change throughout the experiment, indicating a strong adaptive immune response to the vaccination.

VSV-KFDV vaccine induced T_H1-biased $CD4^+$ and cytotoxic $CD8^+$ T cell responses

VSV-KFDV vaccinated animals presented with antigen-specific cytokine secretion from both $CD4^+$ (Fig. 1, C and D) and $CD8^+$ (Fig. 1, E and F) T cells before (D0) and after KFDV challenge (D9). We observed a significant increase in tumor necrosis factor (TNF)−α and interferon (IFN)−γ production by $CD4^+$ T cells compared to control group animals suggesting a bias toward T_H1 responses (Fig. 1, C and D) following vaccination (D0) and KFDV challenge (D9). $CD8^+$ T cells presented with an increase of inflammatory cytokines (IFN-γ and TNF-α) (Fig. 1, E and F), the cytotoxic molecule perforin, and the degranulation marker CD107a (fig. S3, A and B), suggesting cytotoxic function. Together, these data indicate that vaccination with VSV-KFDV induced KFDV-specific T cell responses.

VSV-KFDV vaccine protected animals from clinical disease

After challenge, macaques were monitored at least twice daily and were scored for clinical signs following an approved scoring sheet (*9*, *27*). Animals in the VSV-EBOV vaccinated group displayed varying degrees of clinical signs including decreased appetite, piloerection, hunched posture, mild dehydration, muddy mucosal membranes, nasal discharge, irregular respiration, mild facial edema, shivering, and reduced activity (table S1). The clinical scores for the control group animals started to increase around D2 (scores of about 5) and peaked at D6 (scores ranging from approximately 10 to 30) before they began to decline (Fig. 2A). In contrast, animals in the VSV-KFDV vaccinated group showed decreased appetite as the sole clinical sign, which may be the result of frequent anesthesia rather than KFDV infection (table S1). These animals had either no or very low (scores of <3) scores following KFDV challenge (Fig. 2A). All study animals maintained largely normal blood chemistry and hematology parameters (Fig. 2, B and C, and fig. S4). In contrast to the VSV-KFDV vaccinated animals, VSV-EBOV vaccinated animals demonstrated with significantly reduced platelet counts and modestly reduced albumin starting after D3 (Fig. 2, B and C) after KFDV challenge. These abnormal parameters are associated with poor outcome in human KFDV cases (*2*, *6*, *28*).

VSV-KFDV vaccine inhibited KFDV replication in blood and target organs

KFDV viremia was analyzed on serum samples collected on D0, D1, D3, D6, and D9. In VSV-KFDV vaccinated animals, viremia was measured on D1, peaked on D3 (10^5 $TCID_{50}$/ml) and was cleared on D9 (Fig. 2D). In contrast, KFDV was only isolated at one time point post-challenge (D3) in two of the six VSV-KFDV vaccinated

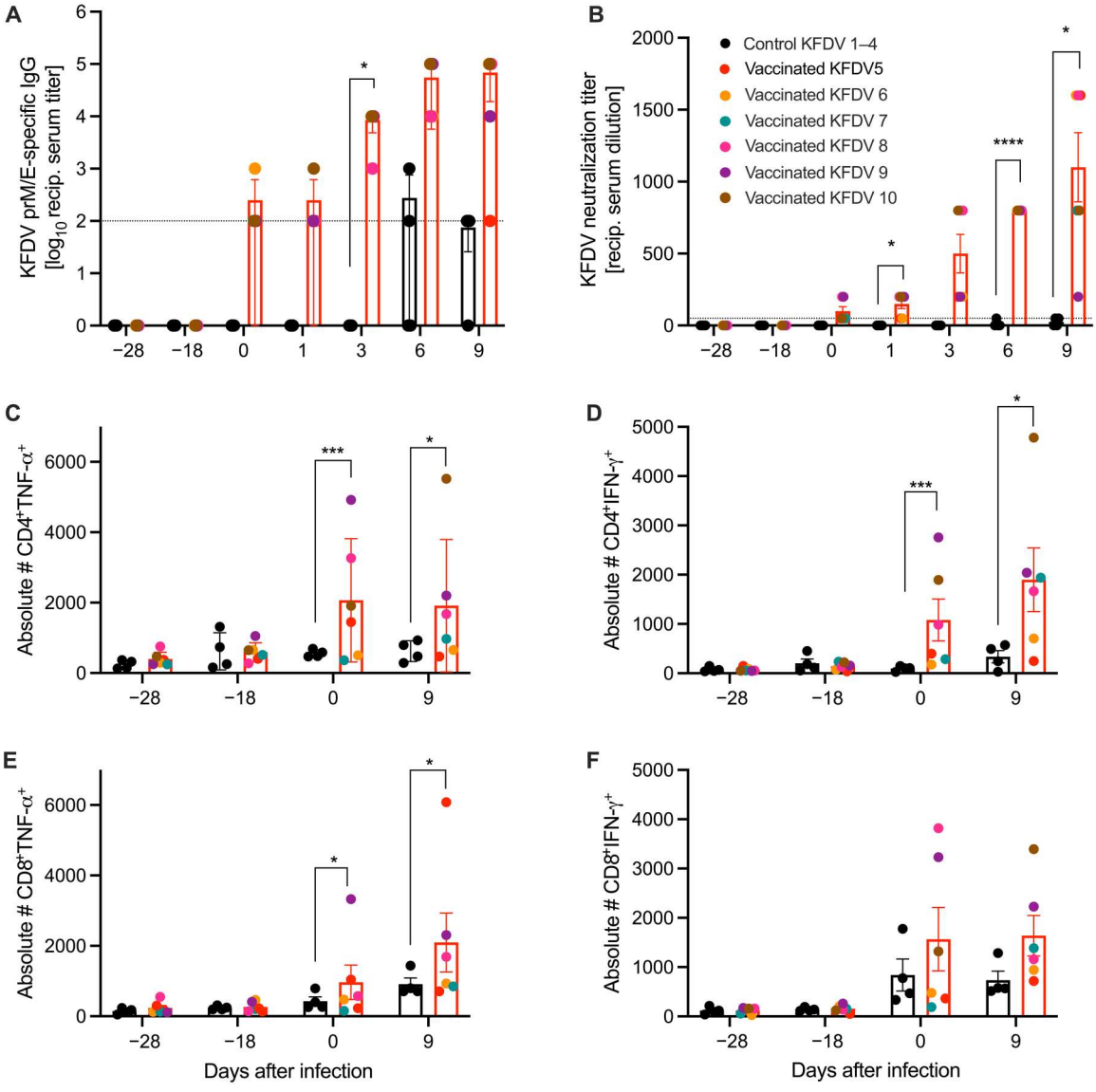

Fig. 1. Adaptive immune responses following VSV-KFDV vaccination and KFDV challenge. (**A**) Total IgG-specific antibodies to KFDV-prM-E were determined by ELISA on serum samples collected from animals immunized with VSV-KFDV (red bars, $n = 6$) and VSV-EBOV (black bars, $n = 4$). Geometric mean and SD are depicted. (**B**) The same serum samples were tested for their neutralizing activity. The highest titer that completely neutralized 100 $TCID_{50}$ of KFDV is shown. (**C** to **F**) VSV-KFDV-specific T cell responses. Cryopreserved PBMCs were stimulated with pooled overlapping peptides derived from the KFDV E protein and analyzed by flow cytometry. All measurements were performed in duplicate for each animal. (C) $CD4^+$TNF-α, (D) $CD4^+$IFN-γ, (E) $CD8^+$TNF-α, and (F) $CD8^+$IFN-γ. Each dot represents a single animal. The dotted line represents the cutoff value of the assay. [(B) to (F)] Mean and SEM are depicted. The dotted line represents assay limit. Statistical significance was analyzed using two-way ANOVA with Sidak's multiple comparisons; results are indicated as $^*P < 0.01$, $^{***}P < 0.001$, and $^{****}P < 0.0001$.

animals (10^3 $TCID_{50}$/ml) (Fig. 2D). Necropsies were performed on D9 to evaluate viral tissue loads and histopathological changes. Guided by the model development study (*9*), we chose different intestinal tissues, cervical lymph nodes, mesenteric lymph node, spleen, and central nervous system (CNS) for the analyses. Infectious KFDV was isolated from the gastrointestinal tissues of most VSV-EBOV vaccinated animals, whereas infectious virus could only be detected in gastrointestinal tissues of a single VSV-KFDV vaccinated animal (Fig. 2E). No live virus was detected in the CNS and spleen. The colon was an exception; all VSV-EBOV vaccinated animals presented with titers between 10^4 and 10^6 $TCID_{50}$ and most VSV-KFDV vaccinated animals with titers around 10^4 $TCID_{50}$ (Fig. 2E).

Gross pathology findings of the VSV-EBOV vaccinated animals included enlarged liver, spleen, and mesenteric lymph nodes as well as hemorrhages in liver, lungs, nasal mucosa, and meninges (table S2). In contrast, VSV-KFDV vaccinated animals presented only mild gross pathology with findings such as a pale liver and ileus in the small intestine of a single animal (table S2). Similarly, KFDV genomic RNA was detected by in situ hybridization (ISH) in the lymphoid tissues of the gastrointestinal tract (stomach, duodenum, jejunum, ileum, cecum, and colon), mesenteric lymph

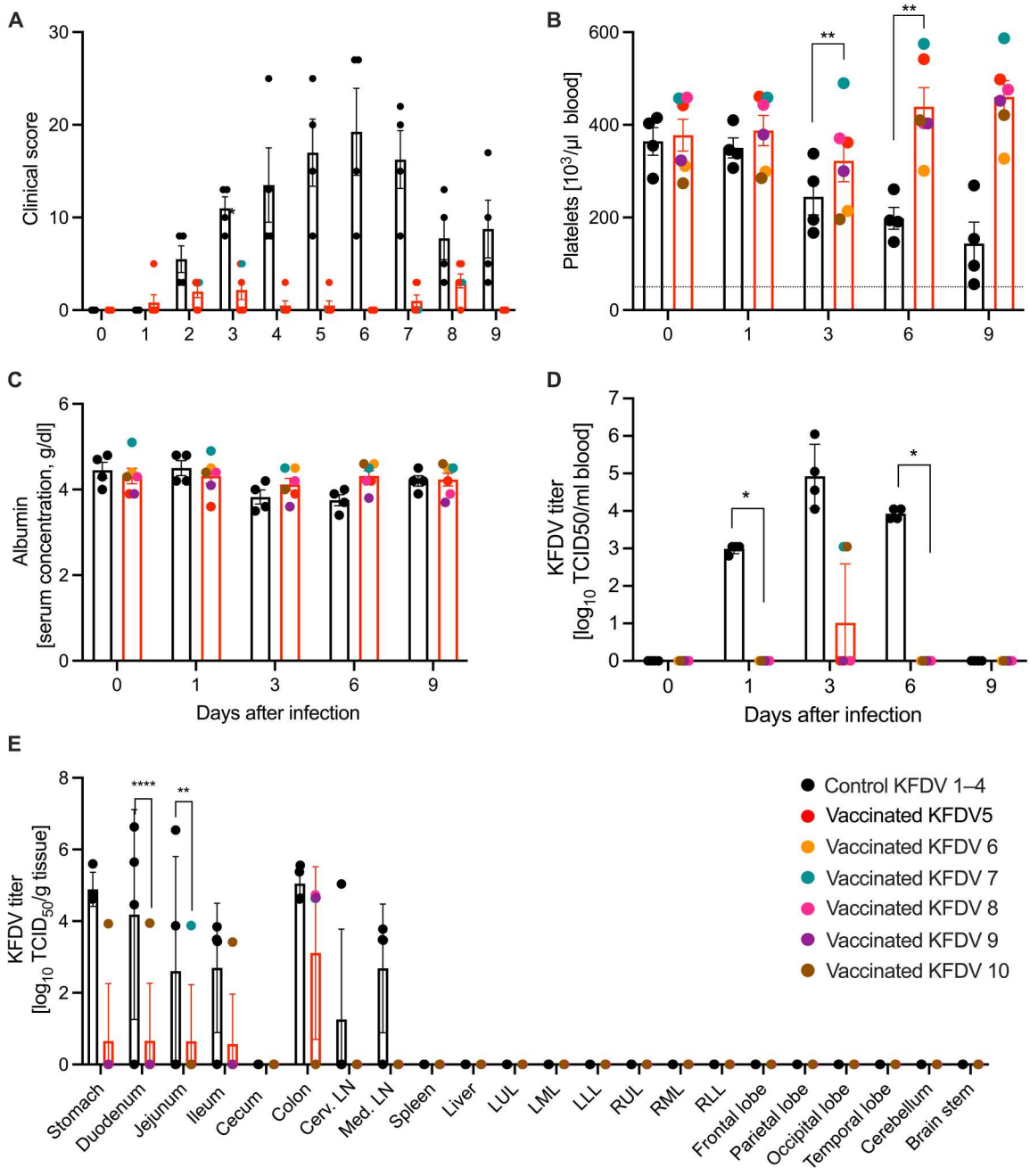

Fig. 2. Clinical, pathophysiologic, and virologic markers of KFDV challenge. (**A**) Animals were monitored daily throughout the study. No clinical signs were observed following vaccination; the scores following KFDV challenge are presented. (**B** and **C**) Blood and serum samples were collected at examination days. EDTA blood was used for hematology and serum was used for blood chemistry. (B) Platelets; (C) albumin. (**D**) EDTA blood samples were used to determine viral titers in blood using a $TCID_{50}$ infectivity assay. [(A) to (E)] Mean and SEM are depicted. (**E**) The study end point was D9 following KFDV challenge when all animals were euthanized and necropsied. Organ titers were determined by a $TCID_{50}$ infectivity assay. Geometric mean and SD are depicted. Statistical significance was analyzed using two-way ANOVA with Sidak's multiple comparisons; results are indicated as $*P < 0.05$, $**P < 0.01$, and $****P < 0.0001$.

node, spleen, and lungs of all VSV-EBOV but not in VSV-KFDV vaccinated animals (Fig. 3). The colon of all VSV-KFDV vaccinated animals showed weak ISH reactivity with diffuse viral genomes that were only visible at higher magnification (fig. S5).

DISCUSSION

Here, we report the development of a live-attenuated VSV-based KFDV vaccine that was safe, elicited strong humoral and cellular immune responses, and provided solid protection against KFD-like disease in two animal disease models, the mouse (*26*) and the pigtailed macaque (this study). This completes the basic preclinical

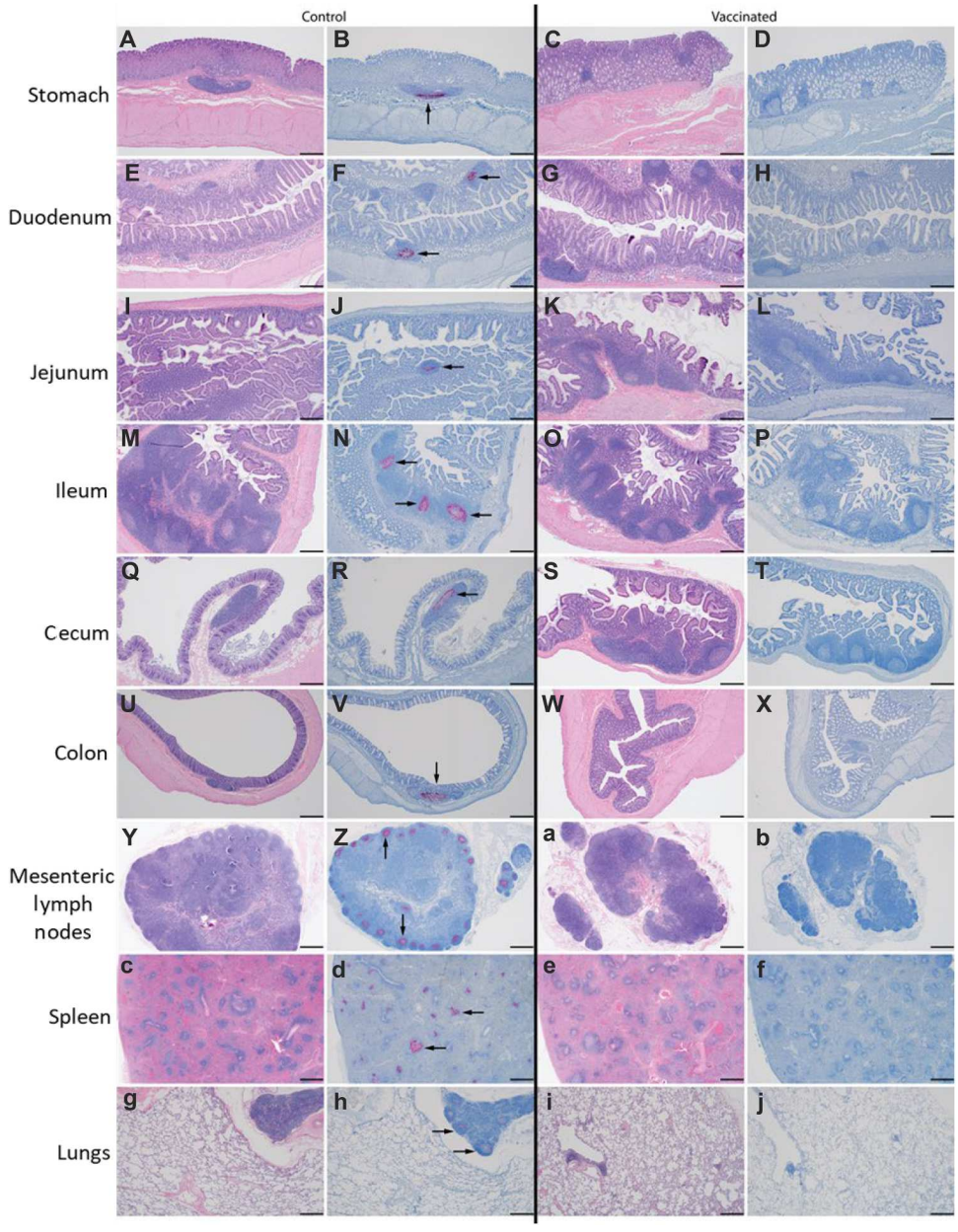

Fig. 3. Detection of KFDV genomic RNA in tissue sections. Animals were euthanized and necropsied at D9 following KFDV challenge (study end point). Formalin-fixed tissue sections were processed for hematoxylin and eosin (H&E) stain and ISH targeting KFDV genome RNA. Representative control (left panel, VSV-EBOV vaccinated) and study (right panel, VSV-KFDV vaccinated) animals are shown: stomach (**A** to **D**), duodenum (**E** to **H**), jejunum (**I** to **L**), ileum (**M** to **P**), cecum (**Q** to **T**), colon (**U** to **X**), mesenteric lymph node (**Y**, **Z**, **a**, and **b**), spleen (**c** to **f**), and lungs (**g** to **j**). Note the presence of genomic signal (black arrows) in the lymphoid follicles of each tissue. The magnification of the images is ×40; the scale bar represents 500μm.

development and allows VSV-KFDV to progress toward clinical development.

Currently, the tissue culture–derived, formalin-inactivated whole virus vaccine is the only KFD vaccine option administered in a two-dose regimen 1 month apart (*23*). However, immunity is short-lived and requires annual booster immunizations. In addition, recent reports of vaccine failures raise concerns and question its future use (*21*, *23*, *29*). Efforts to develop a second-generation vaccine are sparse, challenging public health, which faces expansion of KFDV distribution, increasing KFD case numbers and the existence of variants such as AHFV. There is a promising attempt to develop KFDV E protein–based multi-epitope vaccine candidates using predicted B and T cell epitopes from conserved protein regions. Those candidate KFDV vaccines showed good antigenic properties even with cross-reactivity against AHFV. The vaccine candidates are likely administered as subunit vaccines, but in vivo efficacy data are missing (*30*). Thus, VSV-KFDV is the only second-generation vaccine with good immunogenicity and preclinical efficacy as an option for public health response if clinical trials were to be successful.

One explanation for a reduced efficacy of the formalin-inactivated vaccine is the development of KFDV escape variants. As such, cross-protection against emerging KFDV variants would be of particular interest for a next-generation KFD vaccine. In contrast to a lack of data on cross-protection of the formalin-inactivated vaccine, VSV-KFDV vaccinated macaques in this study clearly generated in vitro cross-reactive neutralizing immune responses to AHFV, a known KFDV variant. This suggests that VSV-KFDV vaccination may elicit cross-protective responses against KFDV variants, but future in vivo experiments need to confirm cross-protective efficacy of VSV-KFDV in animal models against challenge with KFDV variants.

The formalin-inactivated current vaccine has been reported to mainly mediate humoral immunity, indicating that weak T cell responses may be another explanation for reduced efficacy of this vaccine (*31*). Human KFDV infections have been associated with robust T and B cell responses, particularly responses by $CD8^+$ T cells (*31*). The peak of $CD8^+$ T cell activation coincided with the appearance of KFDV-specific IgG leading to KFDV clearance in those patients. In our study, VSV-KFDV vaccination elicited both humoral and T cell–based immunity in the vaccinated macaques and thus may provide stronger and broader protective efficacy than the currently existing formalin-inactivated vaccine (*31*).

Given the infrequent emergence/re-emergence of KFDV in mainly rural areas in India with insufficient health care coverage and logistical difficulties administering vaccines, a single-shot, fast-acting second-generation vaccine would be most beneficial. As such, the VSV platform has multiple benefits over the current multi-boost and slow-acting formalin-inactivated vaccine. As a replication-attenuated vaccine, VSV-KFDV is prone to mediate strong humoral and cellular immune responses following a single vaccination. VSV-EBOV is the prototype VSV-based vaccine and has shown convincing efficacy as a single-shot approach against EBOV infection (*25*). Furthermore, it quickly achieves protective immunity by approximately 1-week post-vaccination in preclinical and clinical applications (*32*, *33*). Therefore, the VSV platform is a promising option for emergency vaccination in remote locations. VSV-KFDV immune response durability following immunization is the subject of further evaluation.

In contrast to VSV-EBOV (*34*), VSV-KFDV is not a monovalent glycoprotein (G) replacement vector. So far, we have not been successful in rescuing this simple replacement vector for KFDV preM/E (*26*) or for Zika virus preM/E (*35*), a mosquito-borne flavivirus. A plausible explanation may be the lack of proper receptor binding and/or fusion for rescue of a monovalent VSV only carrying flavivirus glycoproteins. While most rescuable VSV G replacement vectors carry trimeric class I fusion proteins, flavivirus E proteins are class II fusion proteins and mature through a different cellular pathway (*36*). Thus, incompatibility with VSV in virus structure, particle maturation, and protein function may result in a failure of rescue. On the other hand, VSV-EBOV has demonstrated strong adaptive humoral immune responses likely due to its favorable immune cell targeting mediated through the EBOV GP (*37*). VSV-EBOV is licensed, and clinical toxicity and efficacy data appear promising in humans (*38*). Therefore, this vector is a plausible choice to deliver a second antigen (bivalent VSV-based vectors). This has been successfully achieved previously in preclinical studies for Andes virus (*39*), Nipah virus (*40*), Zika virus (*35*), and SARS-CoV-2 (severe acute respiratory syndrome coronavirus 2) (*41*). This together with the demonstrated preclinical efficacy of VSV-KFDV supports the choice of this strategy.

The KFDV pigtailed macaque model (*9*) is a relatively recent disease model showing certain laboratory blood abnormalities indicative of organ damage (e.g., liver and kidney) and clotting abnormalities resulting in hemorrhages, and edema regularly seen in severe KFD cases (*2*, *9*, *42*, *43*). These parameters are important clinical biomarkers that are often associated with poor outcome in KFD cases. Nevertheless, the pigtailed macaque model may not be perfectly suited for countermeasure efficacy studies as it does not uniformly progress to severe disease. More disease severity and higher lethality may be achieved with alternative nonhuman primate species such as bonnet macaques or black-faced langurs (*4*), but those animals are not widely available for experimental studies. Even pigtailed macaques have limited availability for experimental use, making it difficult to design strongly powered studies with balanced sex and age distribution as experienced in our study here with only female animals being available to us. Therefore, future efforts may have to focus on better defining the pigtailed macaque model and on developing alternative animal models for KFDV.

In summary, our data have demonstrated that the VSV-KFDV vaccine was well tolerated, mediated strong adaptive immune responses, and provided strong protection against KFDV infection in a rodent (*26*) and nonhuman primate KFD-like disease model. This vaccine is well-suited to fill the gap for a proper public health response to a neglected, expanding emerging disease and is ready to enter clinical development.

MATERIALS AND METHODS

Biosafety and ethics

All infectious work with VSV and KFDV was performed in the BSL2 and BSL4 laboratories at the Rocky Mountain Laboratories (RML), Division of Intramural Research (DIR), National Institute of Allergy and Infectious Disease (NIAID), National Institutes of Health (NIH), respectively. All sample processing and sample removals followed standard operating protocols (SOPs) for BSL4 approved by the Institutional Biosafety Committee (IBC). All experiments involving pigtailed macaques were performed in strict accordance with approved Institutional Animal Care and Use Committee protocols and followed recommendations from the *Guide for the Care and Use of Laboratory Animals* of the Office of Animal Welfare, NIH and the Animal Welfare Act of the U.S. Department of Agriculture, in an Association for Assessment and Accreditation of Laboratory Animal Care International–accredited facility. Pigtailed macaques were placed in a climate-controlled room with a fixed 12-hour light-dark cycle. Animals were single housed in adjacent primate cages allowing social interactions and were provided with commercial monkey chow, treats, and fruit twice daily and with water ad libitum. Environmental enrichment was provided with a variety of human interactions, manipulanda, commercial toys, movies, and music. Macaques were monitored at least twice daily throughout the study by trained staff under the supervision of board-certified clinical veterinarians.

Cells

VeroE6 (African green monkey kidney) cells (ATCC CCL-81, Washington, DC, USA) were propagated in Dulbecco's modified

Eagle's medium (DMEM) (Sigma-Aldrich, St. Louis, MO, USA) containing 2 or 10% fetal bovine serum (FBS) (Wisent Inc., St. Bruno, Canada), 2 mM L-glutamine (Thermo Fisher Scientific, Waltham, MA, USA), penicillin (50 U/ml; Thermo Fisher Scientific, Waltham, MA, USA), and streptomycin (50 μg/ml; Thermo Fisher Scientific, Waltham, MA, USA). The cells were incubated at 37°C and 5% CO_2. Cell lines and viral stocks were tested regularly for mycoplasma contamination and were found to be negative.

Viruses

The KFDV strain P9605 (Genbank accession number JF416958; https://www.ncbi.nlm.nih.gov/nuccore/JF416958) was obtained from the University of Texas Medical Branch. KFDV was propagated one time on VeroE6 cells, titrated using a $TCID_{50}$ assay, and sequence confirmed. VSV-KFDV (passage 2) and VSV-EBOV (passage 2) vectors were previously generated in-house on Vero cells and titrated using a PFU assay (*26*, *44*).

Peptide library

Peptides spanning the full-length KFDV E protein sequence were used in antigen-specific T cell assays (Genscript, NJ, USA). A total of 62 peptides were synthesized as 15-mers overlapping by seven amino acids. Five peptides needed to be shortened to 13 amino acids to be successfully synthesized.

Animal study

Pigtailed macaques have limited availability for experimental use, making it difficult to design strongly powered studies with balanced sex and age distribution. Only female pigtailed macaques were available to us for our study. Ten female pigtailed macaques (*M. nemestrina*; 10 to 16 years of age) were randomly assigned to the VSV-KFDV ($n = 6$) and the VSV-EBOV ($n = 4$) group. Animals in the VSV-KFDV group were vaccinated intramuscularly with 1×10^7 PFU of VSV-KFDV on day −28 (D−28) (1 ml and injected into two sites of the caudal thighs). Animals in the VSV-EBOV control group were intramuscularly vaccinated at the same time with 1×10^7 PFU of VSV-EBOV. On D0, all animals were challenged with 2×10^5 $TCID_{50}$ KFDV by a combination of the subcutaneous [1×10^5 $TCID_{50}$ KFDV; four different sites (250 μl each) in the subscapular region] and intravenous [1×10^5 $TCID_{50}$ KFDV; saphenous, cephalic, or femoral vein (1 ml)] routes. Clinical examinations were performed on D−28, D−27, D−25, D−18, D0, D1, D3, D6, and D9 including a full-body evaluation and a venous blood draw for virology, immunology, hematology, and blood chemistry. Swab samples (oral, nasal, and rectal) were collected on D−28, D−27, D−25, D−18, and D0 to analyze VSV viral shedding. Clinical scoring of non-anesthetized animals was performed by an experienced researcher blinded to the study. All hands-on procedures were performed by board-certified clinical veterinarians on anesthetized animals. Necropsies were performed on all euthanized animals by board-certified veterinary pathologists blinded to the study groups. The group sizes were determined with the assumption that all VSV-EBOV vaccinated animals will display clinical signs and reach high KFDV organ/blood loads, and only one of the VSV-KFDV vaccinated animals will display clinical signs and show high KFDV organ/blood loads with the rest of the animals in this group showing no clinical signs and reduced KFDV organ/blood loads (>3 log10 reduction). Using the "Fisher Exact Test Calculator," four VSV-EBOV and six VSV-KFDV vaccinated animals would give a P value of 0.0476, a result that was significant at $P < 0.05$.

Enzyme-linked immunosorbent assay

For the detection of KFDV-specific IgG antibody responses, enzyme-linked immunosorbent assay (ELISA) antigen was prepared by transfecting 293-T (ATCC CRL-3216, Washington, DC, USA) cells with an unaltered pCAGGS plasmid (control) or a pCAGGS plasmid expressing KFDV prM and E proteins. At 24 hours after transfection, cells were lysed with radioimmunoprecipitation assay buffer (Thermo Fisher Scientific, Waltham, MA, USA) and diluted in phosphate-buffered saline (PBS) (*26*). For the detection of EBOV-specific IgG antibody responses, purified EBOV GP was used (*45*). AHFV-specific IgG was detected using concentrated AHFV lysed with Triton X-100. ELISA plates (96-well flat bottom, NUNC, Waltham, MA, USA) were coated with 100 μl (1 ng/μl) of the antigens at 4°C overnight and blocked for 1 hour at room temperature with 5% powdered milk in PBS and 0.05% Tween 20 (Thermo Fisher Scientific, Waltham, MA, USA) (PBST). Subsequently, serial dilutions (1:100 then 10-fold dilutions) of macaque sera in PBST were added to the plate and incubated for 1 hour at room temperature. Detection was performed using anti-mouse IgG coupled with horseradish peroxidase (Jackson ImmunoResearch, PA, USA) for 1 hour at room temperature followed by adding ABTS substrate solution (Seracare, MA, USA) for 15 min at room temperature. Plates were read at 405 nm using a Synergy HTX, Biotek reader (Agilent, CA, USA). Note that for the evaluation and interpretation of KFDV-specific ELISA, the OD_{405} (optical density at 405 nm) of the control antigen-coated wells was subtracted from that of the KFDV antigen-coated wells. Negative results were assigned the value "1."

Virus neutralization assay

Serum from vaccinated and infected macaques was inactivated by gamma-irradiation with a dose of 10 megarad (*46*) and heat-inactivated at 55°C for 30 min. Fourfold serial dilutions of the serum were incubated with 100 $TCID_{50}$ of KFDV or AHFV for 1 hour at 37°C followed by infection of confluent VeroE6 cells. Cytopathic effect was monitored for 96 hours after infection. Neutralization titers were described as the highest titer that completely neutralized 100 $TCID_{50}$ of KFDV or AHFV. The initial dilution of sera was 1:50, which was set as the limit of detection for the assay. Negative results were assigned the value "0." Titers shown represent the average of three independent experiments, each performed with technical replicates.

T cell activation assay

Peripheral blood mononuclear cells (PBMCs) were stimulated with peptides spanning the entire KDFV E protein at a final concentration of 5 μg/ml or dimethyl sulfoxide as a negative control. As a positive control, cells were stimulated with phorbol 12-myristate 13-acetate (50 ng/ml; Sigma) and ionomycin (1 μg/ml; Merck Calbiochem). PBMCs were stimulated for 6 hours in the presence of Brefeldin A (1×; eBioscience) at 37°C, 5% CO_2 and stained for either extracellular or intracellular flow cytometry. For extracellular staining, PBMCs were stained with BV-650 anti-CD3 (catalog #563916, BD Biosciences, dilution 1/200), APC anti-CD4 (catalog #551980, BD Biosciences, dilution 1/200), and PerCP/Cyanine5.5 anti-CD8 (catalog #344710, BioLegend, dilution 1/200) for 30 min at 4°C.

For intracellular staining, the cells were stained with fluorescein isothiocyanate anti-Perforin (catalog no. 3465–7, MabTech, Stockholm, Sweden; dilution 1/50), BV786 anti-CD107a (catalog no. 328644, BioLegend, CA, USA; dilution 1/50), APC/Cyanine7 anti-TNF-α (catalog no. 502944, BioLegend, CA, USA; dilution 1/50), PE/Cyanine7 anti-IFN-γ (catalog no. 502528, BioLegend, CA, USA; dilution 1/50), and BV421 anti-Ki67 (catalog no.151208, BioLegend, CA, USA; dilution 1/100) for 45 min at room temperature in permeabilization wash buffer (eBioscience, Thermo Fisher Scientific, MA, USA). Cells were washed twice with PBS 1× and fixed overnight in 2.5% paraformaldehyde (PFA), pelleted and resuspended in 0.5 ml of fresh 2.5% PFA, and then transferred in a 2-ml cryotube before removal from BSL-4. The samples were analyzed using the BD FACS Symphony instrument (BD Biosciences, NJ, USA) and FlowJo v10. Single-fluorochrome compensation was calculated on beads (catalog no. 01–2222-42, Thermo Fisher Scientific, MA, USA). Peptide-specific responses were calculated by subtraction of the unstimulated controls from the peptide-stimulated samples.

Hematology and blood chemistry

Hematology analysis was completed on a ProCyte DX (IDEXX Laboratories, Westbrook, ME, USA), and the following parameters were evaluated: red blood cells, hemoglobin, hematocrit, mean corpuscular volume, mean corpuscular hemoglobin, mean corpuscular hemoglobin concentration, red cell distribution width, platelets, mean platelet volume, white blood cells, neutrophil count (abs and %), lymphocyte count (abs and %), monocyte count (abs and %), eosinophil count (abs and %), and basophil count (abs and %). Serum chemistry levels were determined on a VetScan VS2 Chemistry Analyzer (Abaxis, Union City, CA, USA) and the following parameters were evaluated: glucose, blood urea nitrogen, creatinine, calcium, albumin, total protein, alanine aminotransferase, aspartate aminotransferase, alkaline phosphatase, total bilirubin, globulin, sodium, potassium, chloride, and total carbon dioxide.

Histopathology

Tissue specimens (<30 mg) were fixed by immersion in 10% neutral buffered formalin for a minimum of 7 days before removal from biocontainment. Tissues were processed with a Sakura VIP-6 Tissue Tek on a 12-hour automated schedule using a graded series of ethanol, xylene, and paraffin. Chromogenic detection of KFDV genomic RNA was performed using the RNAscope VS Universal AP assay (Advanced Cell Diagnostics Inc.) on the Ventana Discovery ULTRA STAINER using a probe targeting the KFDV genome sequence at position 7597–8486 (Advanced Cell Diagnostics Inc. catalog no. 591199). ISH was performed according to the manufacturer's instructions. Histological examinations were performed by a board-certified veterinary pathologist blinded to the study.

Tissue viral loads

Tissue samples were homogenized in 1 ml of plain DMEM with a stainless steel bead at 30 Hz for 10 min using a Tissue Lyser II (Qiagen). Clear homogenate was separated from tissue debris at 8000 rpm for 10 min. Serial dilutions (10-fold) of tissue homogenate were prepared in DMEM and inoculated onto confluent wells of VeroE6 cells in triplicate. The cytopathic effect was monitored for 96 hours after inoculation and $TCID_{50}$ was calculated for each sample using the Reed and Muench method (*47*).

Statistical analysis

All statistical analysis was performed in Prism 9 (GraphPad). Data were examined using two-way analysis of variance (ANOVA) with Sidak's multiple comparisons test to evaluate statistical significance for all samples at all time points. Statistically significant differences are indicated as follows: $^{****}P < 0.0001$, $^{***}P < 0.001$, $^{**}P < 0.01$, and $^{*}P < 0.05$.

Supplementary Materials

This PDF file includes:

Figs. S1 to S5
Tables S1 and S2

REFERENCES AND NOTES

1. T. H. Work, Russian spring-summer virus in India: Kyasanur Forest disease. *Prog. Med. Virol.* **1**, 248–279 (1958).
2. S. Z. Shah, B. Jabbar, N. Ahmed, A. Rehman, H. Nasir, S. Nadeem, I. Jabbar, Z. U. Rahman, S. Azam, Epidemiology, pathogenesis, and control of a tick-borne disease–Kyasanur Forest disease: Current status and future directions. *Front. Cell. Infect. Microbiol.* **8**, 149 (2018).
3. Kyasanur Forest Disease. *Centers For Disease Control and Prevention* (2013). https://cdc.gov/vhf/kyasanur/index.html.
4. M. R. Holbrook, Kyasanur forest disease. *Antiviral Res.* **96**, 353–362 (2012).
5. Select Agents and Toxins List; Centers for Disease Control and Prevention (2023); https://www.selectagents.gov/sat/list.htm
6. B. Bhatia, H. Feldmann, A. Marzi, Kyasanur Forest disease and Alkhurma hemorrhagic fever virus-two neglected zoonotic pathogens. *Microorganisms* **8**, 1406 (2020).
7. R. Stone, Monkey fever unbound. *Science* **345**, 130-1, 133 (2014).
8. T. H. Work, H. Trapido, Summary of preliminary report of investigations of the Virus Research Centre on an epidemic disease affecting forest villagers and wild monkeys of Shimoga District, Mysore. *Indian J. Med. Sci.* **11**, 341–342 (1957).
9. R. M. Broeckel, F. Feldmann, K. L. McNally, A. I. Chiramel, G. L. Sturdevant, J. M. Leung, P. W. Hanley, J. Lovaglio, R. Rosenke, D. P. Scott, G. Saturday, F. Bouamr, A. L. Rasmussen, S. J. Robertson, S. M. Best, A pigtailed macaque model of Kyasanur Forest disease virus and Alkhurma hemorrhagic disease virus pathogenesis. *PLOS Pathog.* **17**, e1009678 (2021).
10. K. A. Dodd, B. H. Bird, M. L. Khristova, C. G. Albarino, S. A. Carroll, J. A. Comer, B. R. Erickson, P. E. Rollin, S. T. Nichol, Ancient ancestry of KFDV and AHFV revealed by complete genome analyses of viruses isolated from ticks and mammalian hosts. *PLOS Negl. Trop. Dis.* **5**, e1352 (2011).
11. R. Mehla, S. R. P. Kumar, P. Yadav, P. V. Barde, P. N. Yergolkar, B. R. Erickson, S. A. Carroll, A. C. Mishra, S. T. Nichol, D. T. Mourya, Recent ancestry of Kyasanur Forest disease virus. *Emerg. Infect. Dis.* **15**, 1431–1437 (2009).
12. P. D. Yadav, S. Patil, S. M. Jadhav, D. A. Nyayanit, V. Kumar, S. Jain, J. Sampath, D. T. Mourya, S. S. Cherian, Phylogeography of Kyasanur Forest disease virus in India (1957-2017) reveals evolution and spread in the Western Ghats region. *Sci. Rep.* **10**, 1966 (2020).
13. K. A. Dowd, S.-Y. Ko, K. M. Morabito, E. S. Yang, R. S. Pelc, C. R. DeMaso, L. R. Castilho, P. Abbink, M. Boyd, R. Nityanandam, D. N. Gordon, J. R. Gallagher, X. Chen, J.-P. Todd, Y. Tsybovsky, A. Harris, Y.-J. S. Huang, S. Higgs, D. L. Vanlandingham, H. Andersen, M. G. Lewis, R. De La Barrera, K. H. Eckels, R. G. Jarman, M. C. Nason, D. H. Barouch, M. Roederer, W.-P. Kong, J. R. Mascola, T. C. Pierson, B. S. Graham, Rapid development of a DNA vaccine for Zika virus. *Science* **354**, 237–240 (2016).
14. N. Pardi, M. J. Hogan, R. S. Pelc, H. Muramatsu, H. Andersen, C. R. DeMaso, K. A. Dowd, L. L. Sutherland, R. M. Scearce, R. Parks, W. Wagner, A. Granados, J. Greenhouse, M. Walker, E. Willis, J. S. Yu, C. E. McGee, G. D. Sempowski, B. L. Mui, Y. K. Tam, Y. J. Huang, D. Vanlandingham, V. M. Holmes, H. Balachandran, S. Sahu, M. Lifton, S. Higgs, S. E. Hensley, T. D. Madden, M. J. Hope, K. Kariko, S. Santra, B. S. Graham, M. G. Lewis, T. C. Pierson, B. F. Haynes, D. Weissman, Zika virus protection by a single low-dose nucleoside-modified mRNA vaccination. *Nature* **543**, 248–251 (2017).
15. D. Betancourt, N. M. G. P. de Queiroz, T. Xia, J. Ahn, G. N. Barber, Cutting edge: Innate immune augmenting vesicular stomatitis virus expressing zika virus proteins confers protective immunity. *J. Immunol.* **198**, 3023–3028 (2017).

16. J. E. Hazlewood, D. J. Rawle, B. Tang, K. Yan, L. J. Vet, E. Nakayama, J. Hobson-Peters, R. A. Hall, A. Suhrbier, A zika vaccine generated using the chimeric insect-specific Binjari virus platform protects against fetal brain infection in pregnant mice. *Vaccines (Basel)* **8**, 496 (2020).
17. K. Raviprakash, K. R. Porter, T. J. Kochel, D. Ewing, M. Simmons, I. Phillips, G. S. Murphy, W. R. Weiss, C. G. Hayes, Dengue virus type 1 DNA vaccine induces protective immune responses in rhesus macaques. *J. Gen. Virol.* **81**, 1659–1667 (2000).
18. J. R. Danko, T. Kochel, N. Teneza-Mora, T. C. Luke, K. Raviprakash, P. Sun, M. Simmons, J. E. Moon, R. De La Barrera, L. J. Martinez, S. J. Thomas, R. T. Kenney, L. Smith, K. R. Porter, Safety and immunogenicity of a tetravalent dengue DNA vaccine administered with a cationic lipid-based adjuvant in a phase 1 clinical trial. *Am. J. Trop. Med. Hyg.* **98**, 849–856 (2018).
19. E. Konishi, M. Yamaoka, I. Kurane, P. W. Mason, A DNA vaccine expressing dengue type 2 virus premembrane and envelope genes induces neutralizing antibody and memory B cells in mice. *Vaccine* **18**, 1133–1139 (2000).
20. Z. Sheng, H. Chen, K. Feng, N. Gao, R. Wang, P. Wang, D. Fan, J. An, Electroporation-mediated immunization of a candidate DNA vaccine expressing dengue virus serotype 4 prM-E antigen confers long-term protection in mice. *Virol. Sin.* **34**, 88–96 (2019).
21. S. K. Kiran, A. Pasi, S. Kumar, G. S. Kasabi, P. Gujjarappa, A. Shrivastava, S. Mehendale, L. S. Chauhan, K. F. Laserson, M. Murhekar, Kyasanur Forest disease outbreak and vaccination strategy,Shimoga District, India, 2013–2014. *Emerg. Infect. Dis.* **21**, 146–149 (2015).
22. A. Oliveira, K. Selvaraj, J. P. Tripathy, U. Betodkar, J. Cacodcar, A. Wadkar, Kyasanur Forest Disease vaccination coverage and its perceived barriers in Goa, India—A mixed methods operational research. *PLOS ONE* **14**, e0226141 (2019).
23. G. S. Kasabi, M. V. Murhekar, V. K. Sandhya, R. Raghunandan, S. K. Kiran, G. H. Channabasappa, S. M. Mehendale, Coverage and effectiveness of Kyasanur forest disease (KFD) vaccine in Karnataka, South India, 2005-10. *PLOS Negl. Trop. Dis.* **7**, e2025 (2013).
24. R. N. Charrel, A. M. Zaki, H. Attoui, M. Fakeeh, F. Billoir, A. I. Yousef, R. de Chesse, P. De Micco, E. A. Gould, X. de Lamballerie, Complete coding sequence of the Alkhurma virus, a tick-borne flavivirus causing severe hemorrhagic fever in humans in Saudi Arabia. *Biochem. Biophys. Res. Commun.* **287**, 455–461 (2001).
25. S. M. Jones, H. Feldmann, U. Stroher, J. B. Geisbert, L. Fernando, A. Grolla, H. D. Klenk, N. J. Sullivan, V. E. Volchkov, E. A. Fritz, K. M. Daddario, L. E. Hensley, P. B. Jahrling, T. W. Geisbert, Live attenuated recombinant vaccine protects nonhuman primates against Ebola and Marburg viruses. *Nat. Med.* **11**, 786–790 (2005).
26. B. Bhatia, K. Meade-White, E. Haddock, F. Feldmann, A. Marzi, H. Feldmann, A live-attenuated viral vector vaccine protects mice against lethal challenge with Kyasanur Forest disease virus. *NPJ Vaccines* **6**, 152 (2021).
27. D. L. Brining, J. S. Mattoon, L. Kercher, R. A. LaCasse, D. Safronetz, H. Feldmann, M. J. Parnell, Thoracic radiography as a refinement methodology for the study of H1N1 influenza in cynomologus macaques (*Macaca fascicularis*). *Comp. Med.* **60**, 389–395 (2010).
28. A. Munivenkatappa, R. R. Sahay, P. D. Yadav, R. Viswanathan, D. T. Mourya, Clinical & epidemiological significance of Kyasanur forest disease. *Indian J. Med. Res.* **148**, 145–150 (2018).
29. P. Rajaiah, Kyasanur Forest Disease in India: Innovative options for intervention. *Hum. Vaccin. Immunother.* **15**, 2243–2248 (2019).
30. S. Arumugam, P. Varamballi, In-silico design of envelope based multi-epitope vaccine candidate against Kyasanur forest disease virus. *Sci. Rep.* **11**, 17118 (2021).
31. S. Devadiga, A. K. McElroy, S. G. Prabhu, G. Arunkumar, Dynamics of human B and T cell adaptive immune responses to Kyasanur Forest disease virus infection. *Sci. Rep.* **10**, 15306 (2020).
32. A. Marzi, S. J. Robertson, E. Haddock, F. Feldmann, P. W. Hanley, D. P. Scott, J. E. Strong, G. Kobinger, S. M. Best, H. Feldmann, EBOLA VACCINE. VSV-EBOV rapidly protects macaques against infection with the 2014/15 Ebola virus outbreak strain. *Science* **349**, 739–742 (2015).
33. A. M. Henao-Restrepo, I. M. Longini, M. Egger, N. E. Dean, W. J. Edmunds, A. Camacho, M. W. Carroll, M. Doumbia, B. Draguez, S. Duraffour, G. Enwere, R. Grais, S. Gunther, S. Hossmann, M. K. Konde, S. Kone, E. Kuisma, M. M. Levine, S. Mandal, G. Norheim, X. Riveros, A. Soumah, S. Trelle, A. S. Vicari, C. H. Watson, S. Keita, M. P. Kieny, J. A. Rottingen, Efficacy and effectiveness of an rVSV-vectored vaccine expressing Ebola surface glycoprotein: Interim results from the Guinea ring vaccination cluster-randomised trial. *Lancet* **386**, 857–866 (2015).
34. M. Garbutt, R. Liebscher, V. Wahl-Jensen, S. Jones, P. Moller, R. Wagner, V. Volchkov, H. D. Klenk, H. Feldmann, U. Stroher, Properties of replication-competent vesicular stomatitis virus vectors expressing glycoproteins of filoviruses and arenaviruses. *J. Virol.* **78**, 5458–5465 (2004).
35. J. Emanuel, J. Callison, K. A. Dowd, T. C. Pierson, H. Feldmann, A. Marzi, A VSV-based Zika virus vaccine protects mice from lethal challenge. *Sci. Rep.* **8**, 11043 (2018).
36. Y. Modis, Class II fusion proteins. *Adv. Exp. Med. Biol.* **790**, 150–166 (2013).
37. J. Prescott, B. L. DeBuysscher, F. Feldmann, D. J. Gardner, E. Haddock, C. Martellaro, D. Scott, H. Feldmann, Single-dose live-attenuated vesicular stomatitis virus-based vaccine protects African green monkeys from Nipah virus disease. *Vaccine* **33**, 2823–2829 (2015).
38. S. T. Agnandji, A. Huttner, M. E. Zinser, P. Njuguna, C. Dahlke, J. F. Fernandes, S. Yerly, J. A. Dayer, V. Kraehling, R. Kasonta, A. A. Adegnika, M. Altfeld, F. Auderset, E. B. Bache, N. Biedenkopf, S. Borregaard, J. S. Brosnahan, R. Burrow, C. Combescure, J. Desmeules, M. Eickmann, S. K. Fehling, A. Finckh, A. R. Goncalves, M. P. Grobusch, J. Hooper, A. Jambrecina, A. L. Kabwende, G. Kaya, D. Kimani, B. Lell, B. Lemaitre, A. W. Lohse, M. Massinga-Loembe, A. Matthey, B. Mordmuller, A. Nolting, C. Ogwang, M. Ramharter, J. Schmidt-Chanasit, S. Schmiedel, P. Silvera, F. R. Stahl, H. M. Staines, T. Strecker, H. C. Stubbe, B. Tsofa, S. Zaki, P. Fast, V. Moorthy, L. Kaiser, S. Krishna, S. Becker, M. P. Kieny, P. Bejon, P. G. Kremsner, M. M. Addo, C. A. Siegrist, Phase 1 trials of rVSV Ebola vaccine in Africa and Europe. *N. Engl. J. Med.* **374**, 1647–1660 (2016).
39. Y. Tsuda, D. Safronetz, K. Brown, R. LaCasse, A. Marzi, H. Ebihara, H. Feldmann, Protective efficacy of a bivalent recombinant vesicular stomatitis virus vaccine in the Syrian hamster model of lethal Ebola virus infection. *J. Infect. Dis.* **204**Suppl 3, S1090–S1097 (2011).
40. B. L. DeBuysscher, D. Scott, A. Marzi, J. Prescott, H. Feldmann, Single-dose live-attenuated Nipah virus vaccines confer complete protection by eliciting antibodies directed against surface glycoproteins. *Vaccine* **32**, 2637–2644 (2014).
41. W. Furuyama, K. Shifflett, A. N. Pinski, A. J. Griffin, F. Feldmann, A. Okumura, T. Gourdine, A. Jankeel, J. Lovaglio, P. W. Hanley, T. Thomas, C. S. Clancy, I. Messaoudi, K. L. O'Donnell, A. Marzi, Rapid protection from COVID-19 in nonhuman primates vaccinated intramuscularly but not intranasally with a single dose of a vesicular stomatitis virus-based vaccine. *mBio* **13**, e0337921 (2022).
42. D. R. Patil, P. D. Yadav, A. Shete, G. Chaubal, S. Mohandas, R. R. Sahay, R. Jain, C. Mote, S. Kumar, H. Kaushal, P. Kore, S. Patil, T. Majumdar, S. Fulari, A. Suryawanshi, M. Kadam, P. G. Pardeshi, R. Lakra, P. Sarkale, D. T. Mourya, Study of Kyasanur forest disease viremia, antibody kinetics, and virus infection in target organs of *Macaca radiata*. *Sci. Rep.* **10**, 12561 (2020).
43. B. Bhatia, E. Haddock, C. Shaia, R. Rosenke, K. Meade-White, A. J. Griffin, A. Marzi, H. Feldmann, Alkhurma haemorrhagic fever virus causes lethal disease in IFNAR$^{-/-}$ mice. *Emerg. Microbes Infect.* **10**, 1077–1087 (2021).
44. A. Marzi, H. Ebihara, J. Callison, A. Groseth, K. J. Williams, T. W. Geisbert, H. Feldmann, Vesicular stomatitis virus-based Ebola vaccines with improved cross-protective efficacy. *J. Infect. Dis.* **204**Suppl 3, S1066–S1074 (2011).
45. E. Nakayama, A. Yokoyama, H. Miyamoto, M. Igarashi, N. Kishida, K. Matsuno, A. Marzi, H. Feldmann, K. Ito, M. Saijo, A. Takada, Enzyme-linked immunosorbent assay for detection of filovirus species-specific antibodies. *Clin. Vaccine Immunol.* **17**, 1723–1728 (2010).
46. F. Feldmann, W. L. Shupert, E. Haddock, B. Twardoski, H. Feldmann, Gamma Irradiation as an effective method for inactivation of emerging viral pathogens. *Am. J. Trop. Med. Hyg.* **100**, 1275–1277 (2019).
47. L. J. Reed, H. Muench, A simple method of estimating fifty per cent endpoints. *Am. J. Epidemiol.* **27**, 493–497 (1938).

Acknowledgments: We wish to acknowledge the Rocky Mountain Laboratories Veterinary Branch, DIR, NIAID, NIH for assistance with animal care and execution of animal studies. We further wish to thank the staff of the Office of the Chief, Laboratory of Virology, DIR, NIAID, NIH, for assistance with high biocontainment operation. We thank A. Mora, Visual and Medical Arts, Research Technologies Branch, DIR, NIAID, NIH for help with graphical design. The opinions, conclusions, and recommendations in this report are those of the authors and do not necessarily represent the official positions of the DIR, NIAID, NIH. **Funding:** The work was funded by the Intramural Research Program of NIAID, NIH. **Author contributions:** Conceptualization: B.B., A.M., and H.F. Methodology: B.B., T.-L.T.-H., F.F., P.W.H., R.R., and C.S. Investigation: B.B., T.-L.T.-H., F.F., P.W.H., R.R., and C.S. Visualization: B.B., A.M., and H.F. Supervision: A.M. and H.F. Resources: A.M. and H.F. Funding acquisition: H.F. Writing—original draft: B.B., A.M., and H.F. Writing—editing and review: B.B., T.-L.T.-H., F.F., P.W.H., R.R., C.S., A.M., and H.F. **Competing interests:** The authors declare that they have no competing interests. **Data and materials availability:** All data needed to evaluate the conclusions in the paper are present in the paper and/or the Supplementary Materials.

Submitted 8 June 2023
Accepted 3 August 2023
Published 6 September 2023
10.1126/sciadv.adj1428